3D3-4

Fully Polarimetric and Interferometric FM-CW SAR System and Its Preliminary Measurement Results

Jun NAKAMURA [1], Kazuyasu AOYAMA [1], Muneyuki IKARASHI [1],
Yoshio YAMAGUCHI [1], Hiroyoshi YAMADA [1]
[1] Dept. of information Engineering, Niigata University
Ikarashi 2-8050, Niigata-shi, 950-2181 Japan
nakamura@wave.ie.niigata-u.ac.jp, yamaguch@ie.niigata-u.ac.jp

1. Intruduction

Radar polarimetry deals with fully polarimetric information of scattered waves from a target. It has been attracting attention in many application areas such as observation of the earth, surveillance for disaster, etc. Airbone or satellite Synthetic Aperture Radar uses the L-band and the X-band as operating frequency, and has the maximum resolution of several meters. In resent years, the Ku-band is expected for next generation SAR because the maximum attainable resolution becomes 30 cm. Based on this situation, we have developed a fully polarimetric FM-CW SAR system in the Ku-band.

In this paper, we present a brief description of fully polarimetric and interferometric FM-CW radar system. The system is then applied to detect coherent change on sandy surface in anechoic chamber. It is shown that the system can measure a slight change on the sandy surface.

2. The FM-CW Pol-InSAR System

We have developed a fully polarimetric FM-CW radar system [1], [2]. Using an FM-CW radar, we can obtain the data easilly compared to the pulse radar or Network Analyzer system.

The scattering matrix can be obtained in fully polarimetric radar mode as shown in Fig. 1. The scattering matrix $[S]$ in the linear polarization basis HV is written as

$$[S] = \begin{bmatrix} S_{HH} & S_{HV} \\ S_{VH} & S_{VV} \end{bmatrix}. \tag{1}$$

We need to change antenna polarization to acquire scattering matrix elements. Since the radar can receive the H and V polarization components simultaneously, a scattering matrix is obtained by switching transmitting antennas. The antenna configuration and the block diagram of fully polarimetric FM-CW

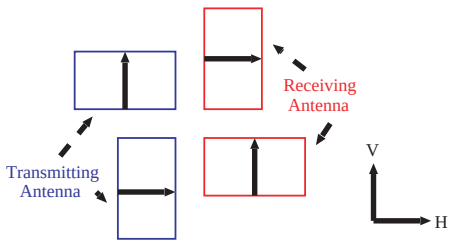

Figure 1: Antenna configuration.

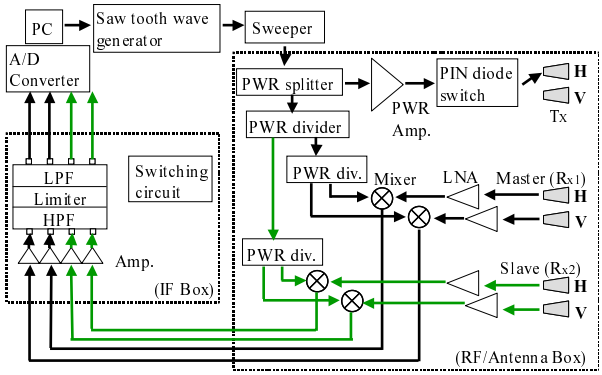

Figure 2: Block diagram of polarimetric and interferometric FM-CW radar.

ISBN: 978-4-88552-223-9 C3055©IEICE

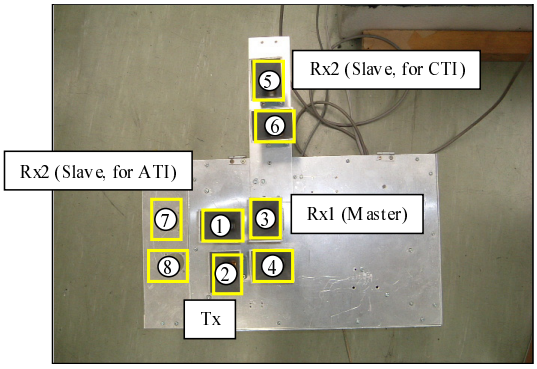

Figure 3: Front panel of RF/Antenna box. There are six antennas for polarimetric and interferometric data acquisition. Slave antenna set is arranged for Cross-Track Interferometry mode.

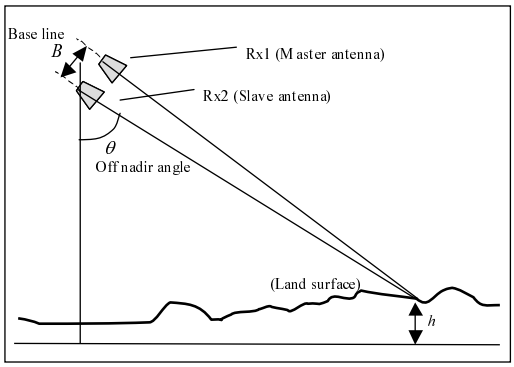

Figure 4: Geometry of Cross-Track Interferometry.

SAR system are shown in Fig. 1 and Fig. 2. This system can obtain scattering matrix elements along a range direction of within 20 ms.

Interferometric radar system has six antennas as shown in Fig. 3. This picture shows the front panel of RF/Antenna box in Fig. 2. These six Ku-band horn antennas on the front panel allow us to obtain the polarimetric and interferometric data. Left two antennas (#1 and 2) are transmitting antennas, T_x, and right four (#3, 4, 5, and 6) are receiving antennas, R_{x1} and R_{x2}. Interferometery uses two close receiving antenna sets named "Master" and "Slave". Antenna 3 and 4 are master antenna set, R_{x1}, in this system. On the other hand, antenna 5 and 6 are slave antenna set, R_{x2}. These two receiving antenna sets allow us to obtain couple of scattering matrices simultaneously. If slave antenna set is located above master antenna like Fig. 3, it is Cross-Track Interferometry suitable for height information retrieval. Fig. 4 shows a geometry of Cross-Track Interferometry. The length B between Master and Slave is the base line in Fig. 4. Angle θ is off nadir angle. If slave antenna set is beside T_x (#7 and 8), the velocity data can be obtained. It is Along-Track Interferometry. The base line is variable in both interferometric modes.

Since the SAR system shown in Fig. 2 is portable, various measurements can be conducted not only in anechoic chamber but also outside easily.

3. Measurement of sandy surface

In this section, we represent the results of a measurement to show that the radar system works as Ku-band Pol-InSAR. The arrangement of antenna sets, Master and Slave, and the target is shown in Fig. 6. The RF/Antenna box was mounted on the X-Y positioner, and scanned 128 cm for SAR processing. The base line is 12 cm and the antenna height is 190 cm. Other measurement parameters are shown in Table 1.

The target is sandy surface in a styrene form boat shown in Fig. 5. Target #1 is flat sandy surface and target #2 is surface with a 30 cm footprint. We put the target 70 cm above the floor to separate the reflections from the floor.

Table 1: Measurement parameter.

Center frequency	15 GHz	Scanning interval	1 cm
Sweep frequency	2 GHz	FFT points	16384
Sweep time	5 ms	Antenna height	190 cm
Scanning points	128	Off nadir angle	45 deg.

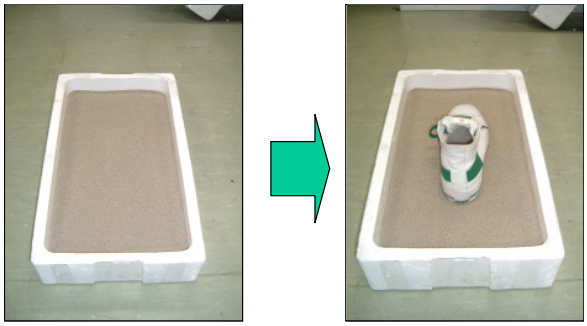

Figure 5: Target #1 is flat sandy surface and #2 is surface with a footprint.

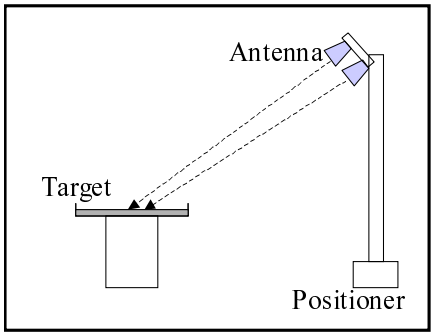

Figure 6: Target arangement (side view).

3. 1 Detection of coherent change using difference

Each data was analyzed simply by using the amplitude and the phase of scattering matrix. First of all, each polarized data (for example, S_{HH}) was analyzed by using the difference before and after leaving a footprint. If radar can measure a coherent change on the sandy surface, some difference is expected in footprint area. The amplitude image of the difference data and the phase image are shown in Fig. 7 and Fig. 8, respectively. $S_{VV\#1}^{master}$ means VV polarized data of target #1 received by master antenna in this paper. The circle in each figure shows footprint area. In Fig. 7, reflection from the floor comes out randomly, so it is difficult to distinguish the footprint. However the difference of phase in footprint area is obviously different from other areas in Fig. 8. Using the difference of the phase, we can find a small change on the sandy surface well.

3. 2 Detection of coherent change using coherence

The footprint area was examined by phase difference between masater and slave. Fig. 9 shows the phase of coherence between $S_{VV\#1}^{master}$ and $S_{VV\#1}^{slave}$. Coherence γ between two comlex value, c_1 and c_2, is defined as

$$\gamma = \frac{\langle c_1 c_2^* \rangle}{\sqrt{\langle |c_1|^2 \rangle \langle |c_2|^2 \rangle}}, \qquad 0 \leqq |\gamma| \leqq 1 \tag{2}$$

where $\langle\rangle$ and $*$ show ensemble average and complex conjugate, respectively [3]. The coherence can be used as a measure for the accuracy of the interferometric phase or as a tool for imaging. The averaging size is 5 pixel in the range by 5 pixel in the azimuth direction.

Both Fig. 9 and Fig. 10 have fringe pattern in range direction. These patterns show that the radar acts as interferometric SAR system. There is no disruption in a fringe pattern in Fig. 9. But in Fig. 10, the pattern disrupted on the footprint. The footprint on the sand is clearly found in Fig. 10 while it is not found in Fig. 9. It is possible to dis tinguish coherent change by this Pol-InSAR system.

4. Conclusions

We have developed a fully polarimetric and interferometric FM-CW radar system operative in the Ku-band. It will serve as a compact radar aimed at developing new Pol-InSAR applications. Through a detection experiment conducted in anechoic chamber, the possibility of full Pol-InSAR system is confirmed.

Acknowledgments

This work in part is carried out by Grant-in-Aid for scientific Research, JSPS, Japan.

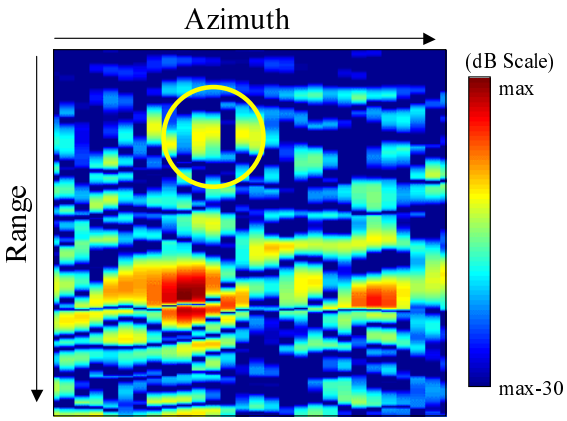

Figure 7: $|(S_{VV\#2}^{master} - S_{VV\#1}^{master})|$.

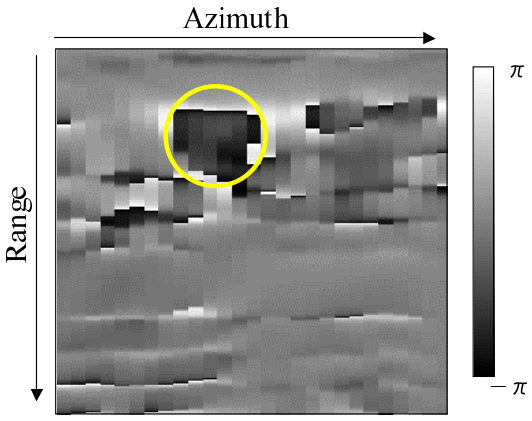

Figure 8: Phase$(S_{VV\#2}^{master} - S_{VV\#1}^{master})$.

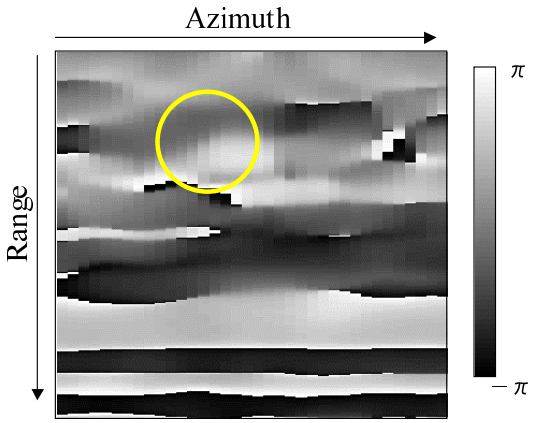

Figure 9: Phase(γ) between $S_{VV\#1}^{master}$ and $S_{VV\#1}^{slave}$.

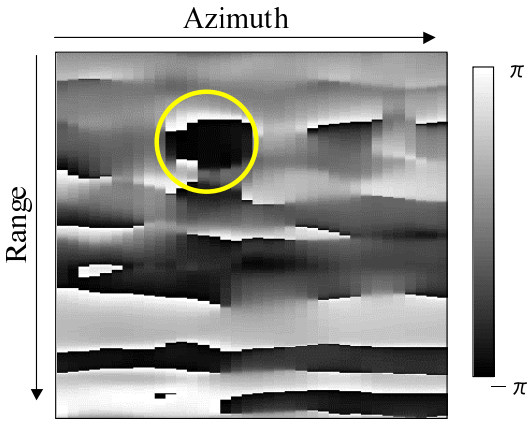

Figure 10: Phase(γ) between $S_{VV\#2}^{master}$ and $S_{VV\#2}^{slave}$.

References

[1] M. Ikarashi, J. Nakamura, K. Aoyama, Y. Yamaguchi, and H. Yamada, “Laboratory Measurements by a Fully Polarimetric FM-CW SAR in the Ku-band, ”, PIERS2006, Tokyo, Japan, pp.175, 2006.

[2] M. Ikarashi, K. Aoyama, J. Nakamura, Yamaguchi, and H. Yamada, “A New FM-CW Pol-InSAR System for Laboratory Measurement, ”, PIERS2006, Tokyo, Japan, pp.174, 2006.

[3] Ramon F. Hanssen, *Radar Interferometery, Data Interpretation and Error Analysis*, Kluwer Academic Publishers, Dordecht, pp.96–98, 2001.